Simulations of the aqueous solvation of trilaurin

ARTICLE *in* JOURNAL OF AGRICULTURAL AND FOOD CHEMISTRY · OCTOBER 1994

Impact Factor: 2.91 · DOI: 10.1021/jf00046a006

3 AUTHORS, INCLUDING:

Søren Balling Engelsen
University of Copenhagen
259 PUBLICATIONS **5,875** CITATIONS

Simulations of the Aqueous Solvation of Trilaurin

Søren B. Engelsen

Chemistry Department A, The Technical University of Denmark, DK-2800 Lyngby, Denmark

John W. Brady* and John W. Sherbon

Institute of Food Science, Cornell University, Ithaca, New York 14853

Molecular dynamics and energy minimization computer modeling calculations have been used to study the conformational behavior of the prototypical triglyceride molecule trilaurin. The energy of an isolated molecule was minimized using both the Quanta/CHARMm force field and a newly developed CFF parametrization for comparisons. The crystal structure was found to be a locally stable geometry using CHARMm, but with the CFF potential the structure collapsed into a geometry with C_3 symmetry similar to the hypothesized bilayer structure with all three aliphatic chains on the same side of the glycerol backbone. A full molecular dynamics simulation of a trilaurin molecule in aqueous solution, starting in the crystal structure, was also performed. This "tuning fork" structure was found to undergo a slow drift in solution toward a more compact geometry, but it was not possible to simulate the system for a sufficient period to determine whether this process was completed or would continue until a geometry similar to the CFF structure was reached. The triglyceride–water interactions were found to be consistent with the behavior expected for a predominantly hydrophobic species containing a polar headgroup consisting of hydrogen-bond-accepting oxygen atoms.

Keywords: *Fat; oil; triglyceride; trilaurin; molecular dynamics; aqueous solution; solvation effects*

INTRODUCTION

Triacylglycerols (triglycerides) are high caloric content neutral lipid molecules found in adipose tissues and plant oils (Small, 1986). Molecules of this class are the primary component of milk fat, and their properties thus dominate the physical properties of foods made from milk fat, such as butter (Mulder and Walstra, 1974). Among the more important of these properties is a smooth, creamy texture, or "mouthfeel", and an ability to solubilize nonpolar or hydrophobic components, including some vitamins and flavor molecules. These textural properties are in turn sensitive to the physical state of the triglycerides, which often have melting points near or above room temperature, with the melting points generally increasing with the length of the saturated fatty acid components.

The simple triglycerides are polymorphous compounds found in three crystalline phases designated α, β', and β. Due to a high degree of conformational flexibility, and thus considerable thermal motions, only two structures, tricaprin (Jensen and Mabis, 1966) and trilaurin (Larsson, 1964; Gibon et al., 1984), have yet been solved to atomic resolution using X-ray diffraction spectroscopy, and both only in the thermodynamically stable β-phase. In both cases the triglyceride crystallizes in a triclinic unit cell, and the monomer structures show a high degree of similarity. The monomer structure can be described as a "tuning fork" or "chair" structure in which the hydrophilic glycerol ester forms the center ("seat"), and all three hydrophobic hydrocarbon chains lie in essentially parallel planes, two pointing in one direction and the third in the opposite (see Figure 1). In the crystal these simple triglycerides pack into a bilayer structure; the interface between the bilayers is stabilized by the formation of a terrace-like arrangement. The carbonyl groups are perfectly antialigned to match another antiparallel monomer, forming the dimeric repeating unit of the crystal. The most remarkable feature in the reported monomer conformations is a measured alternation of the C–C bond lengths and of the C–C–C angles. It has been suggested by Jensen and Mabis (1966) that this pattern may be due to the

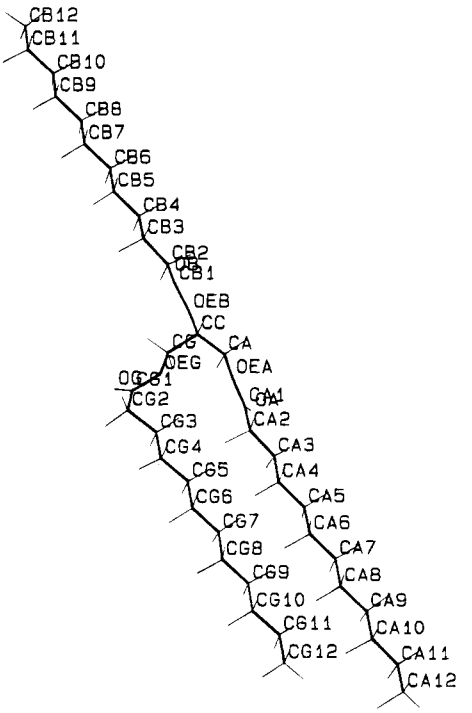

Figure 1. Crystal structure of β-phase trilaurin.

* Author to whom correspondence should be addressed.

0021-8561/94/1442-2099$04.50/0

large thermal anisotropy of the chains and possible rotary oscillation of the chains about their longitudinal axes.

Triglycerides are generally insoluble in water and do not readily form micelles (Small, 1986). Because of their limited aqueous dispersability, triglycerides are usually found in milk as protein-stabilized globules or in buffer as a separate lipid phase. Butter is a complex emulsion consisting of a continuous fat phase resulting from coalescence of the milk fat globules and a dispersed aqueous phase (Mulder and Walstra, 1974). A significant portion of the fat globule membranes are damaged or disrupted in the churning process and are lost in the buttermilk. As a result, water and fat in butter are in direct contact across the emulsion interfaces throughout much of the butter system. For this reason, it would be useful to understand the way in which water and triglycerides interact and how their interactions affect the molecules of each phase.

Little is known about the details of the relationship between molecular structure and the physical properties of the triglycerides. One potential source of such detailed information would be theoretical computer dynamics simulations (Brooks et al., 1988) such as have been extensively applied to small molecules (Burkert and Allinger, 1982), liquids (Allen and Tildesley, 1987), proteins (Brooks et al., 1988), nucleic acids (McCammon and Harvey, 1987), and carbohydrates (French and Brady, 1990). No such dynamics studies have yet been reported of triglycerides, but an interesting recent paper did report semiempirical quantum mechanical and energy minimization studies of triacylglycerols, including trilaurin (Yan et al., 1994). There have also been several recent studies of other lipid systems (Egberts et al., 1988; Pastor et al., 1988; Watanabe and Klein, 1989; Pastor et al., 1991; DeLoof et al., 1991; Raghavan et al., 1992; Nyholm and Pascher, 1993; Venable et al., 1993). We report here preliminary molecular dynamics simulations of the triglyceride trilaurin, both isolated in vacuum and in aqueous solution, in preparation for such simulations of triglyceride crystalline phases.

PROCEDURES

In the studies reported here, models for a simple saturated fat triglyceride in the crystal structure conformation of β-phase trilaurin (Larsson, 1964; Gibon et al., 1984) were subjected to comparative conjugate gradient energy minimization and molecular dynamics simulation *in vacuo* using two different molecular mechanics force fields. The main calculation reported here is a subsequent molecular dynamics simulation of a single trilaurin molecule in an explicit water phase. Trilaurin (Figure 1), $C_{39}H_{74}O_6$ (MW 639.0174), has a crystal density of 1.05 g mol^{-1} and a melting point of 48.1 °C (Larsson, 1964; Gibon et al., 1984). It is formed by the attachment of three lauric acids to glycerol via dehydration. This molecule is the smallest simple triacylglycerol that is typical of long-chain saturated fats in its physical behavior. With its crystal structure carefully detailed, trilaurin is thus a good model for study of the behavior of such triglycerides in water.

In the dynamics studies reported here, Newton's equations of motion were integrated numerically for every atom in the model system using the general purpose molecular mechanics program CHARMM developed by Karplus and co-workers (Brooks et al., 1983). The potential energy functions used were typical molecular mechanics energy functions

$$V(\mathbf{q}) = \sum k_b(b - b_o)^2 + \sum k_\theta(\theta - \theta_o)^2 + \sum k_\phi[1 + \cos(n\phi - \delta)] + \sum k_\omega(\omega - \omega_o)^2 + \sum_{ij}(A_{ij}/r_{ij}^{12} - B_{ij}/r_{ij}^{6} + q_iq_j/D_e r_{ij}) \quad (1)$$

with the dielectric constant D_e equal to 1. Nonbonded 1−4 interactions were scaled by a factor of 0.5. The parameters for the solute were taken from the commercially available Quanta21.3 parameter set (released with the commercial molecular mechanics program package QUANTA v. 21.3 distributed by Molecular Simulations, Inc., Sunnyvale, CA), and the water molecules were modeled using the TIP3P potential energy function (Jorgensen, 1981). The partial charges for the ester groups within the solute were taken from the OPLS potential energy functions (Briggs et al., 1990) to make the electrostatic energies of the solute comparable to the energies of the solvent.

No explicit hydrogen-bonding function was used as these interactions are believed to be modeled adequately by a combination of van der Waals and Coulombic potentials. All hydrogen atoms were explicitly included in the simulation, although all bond lengths involving hydrogen were kept fixed throughout the simulation using the constraint algorithm SHAKE (van Gunsteren and Berendsen, 1977). The valence angles of the solvent molecules also were kept constant.

Minimum-image periodic boundary conditions were applied to the system to mimic condensed phase conditions and to eliminate edge effects. Interactions between atoms more than 12 Å apart were truncated. Switching functions were used to smoothly turn off long-range interactions between 10 and 11 Å. To avoid artificially splitting dipoles at the cutoff border, we applied the switching function on a group-by-group basis, with the groups corresponding to complete water molecules and to electrostatically neutral groups in the solute (3−9 atoms, resulting in 33 groups) (Brooks et al., 1983; Tasaki et al., 1993). Interactions for each atom were thus summed over all of its neighbors in the primary box and all those image neighbors within the cutoff distance. Periodic boundaries were applied to the system as a rectangular box measuring 24.7170 by 24.7170 by 49.7252 Å to give a density of 1.0 g cm^{-3}. This value was chosen arbitrarily since no density data for dilute solutions of trilaurin in water were available. The concentration of the resulting solution was 0.055 M.

The initial coordinates for the system were prepared by superimposing the crystallographic coordinates of a single β-phase trilaurin molecule (Larsson, 1964; Gibon et al., 1984) upon the previously calculated coordinates of a well-equilibrated box of pure TIP3P water. Those water molecules whose van der Waals radii overlapped any of the atoms in the trilaurin solute were deleted from the system, leaving 980 water molecules in the primary box. Initial velocities for all atoms were assigned from a Boltzmann distribution at 300 K, the temperature at which the box of pure water was equilibrated, and their equations of motion were integrated using the two-step velocity Verlet algorithm (Verlet, 1967) with a step size of 1 fs. The system was equilibrated for 10 ps to relax any artificial starting conditions produced by the solvation procedure, with occasional scaling of the atomic velocities when the average temperature deviated from the desired value of 300 K by more than an acceptable tolerance of ±3 K. Following the equilibration period, the integration was continued without further interference for an additional 165 ps period of data collection. Energy was well conserved in the simulation, with the average rms fluctuations in the Hamiltonian divided by those of the kinetic energy being 0.009 when collected in 2 ps intervals of the production dynamics trajectory. The total simulation required approximately 75 CPU days on an IBM RISC 6000 Model 320 minicomputer.

RESULTS AND DISCUSSION

Static Energy Minimization *in Vacuo*. The application of static conformational analysis using molecular mechanics methods to such a flexible molecule as trilaurin is problematic due to the large conformational freedom and the resultant flat energy surface of the conformational space with many shallow local minima. However, since static molecular mechanics methods are fundamental to the development of the molecular mechanics force fields used to perform molecular dynamics simulations, it is of interest to analyze the "strain energy" of the crystal structure using two

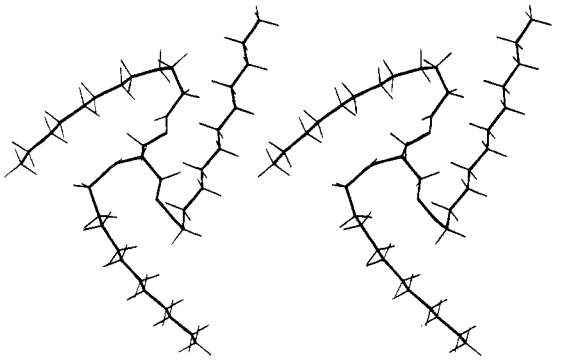

Figure 2. β-Phase structure of trilaurin when minimized in PEF91L.

different force fields, since little attention has been paid to forcefield development for lipids.

The crystal structure of β-phase trilaurin was energy minimized for an isolated molecule using two very different molecular mechanics force fields. One was the Quanta21.3 force field used in the dynamics simulation and described under Procedures. The second force field used was the recently developed PEF91L force field (Engelsen, 1991) intended for future lipid research, which has been optimized using the Consistent Force Field concept (Niketic and Rasmussen, 1977; Rasmussen, 1985). The PEF91L type of force field differs from the Quanta21.3 force field by using Morse potentials for modeling covalent bonds and by using the bond torsional approach instead of the group torsional approach.

Although it is unlikely that the tuning fork structure is the lowest energy vacuum structure, the Quanta21.3 force field preserved this overall structure during energy minimization since it apparently corresponds to a local energy minimum with a small energy barrier prohibiting a transition to more energetically favorable conformations, especially with respect to van der Waals interactions. Surprisingly, when minimized in the PEF91L force field, the tuning fork structure of β-trilaurin changed to a conformation having C_3 symmetry, with the chiral carbon atom (the methine group) in the center and the three hydrocarbon chains forming spirals reaching out from the center (see Figure 2). This structure may also be unlikely to have any significance *in vacuo*, but several minimizations of trial starting structures in which all three chains lay in a unidirectional, parallel arrangement also produced spiral final structures. In their conformational energy studies of 243 possible starting structures, Yan et al. also found that the lowest energy geometry had all three chains aligned on the same side of the glycerol backbone (Yan et al., 1994) but in a roughly parallel geometry similar to that believed to exist in lipid membranes.

Table 1 shows the variations of C–C bond lengths in the crystal and in the minimized structures using both force fields. Using the Quanta21.3 force field, about 70% of the strain was due to distortion in bond lengths, while using the PEF91L force field, the bond strain was calculated to account for only about 50% of the strain energy. As expected, neither of the molecular mechanics force fields was able to reproduce the alternating C–C bond lengths of the hydrocarbon chains observed in the crystal structures of the triglycerides (Jensen and Mabis, 1966; Larsson, 1964; Gibon et al., 1984) as well as in the related glycosphingolipids (Nyholm et al., 1990). Due to the poor statistics of the X-ray structure refinement procedures, the phenomena can only be regarded as being significant in the CA9–CA10–CA11 region (0.045 Å), where the amplitudes of the thermal

Table 1. Trilaurin Bond Lengths:[a] Comparison of Trilaurin C–C Bond Lengths in the Crystal (Gibon et al., 1984) and in the Minimized Structures Using the Two Force Fields Quanta21.3 and PEF91L

bond		X-ray	Quanta21.3	PEF91L
CC	CA	1.496	1.531 (0.035)	1.537 (0.041)
CA	OEA	1.435	1.470 (0.035)	1.441 (0.006)
OEA	CA1	1.331	1.354 (0.023)	1.364 (0.033)
CA1	OA	1.202	1.225 (0.023)	1.214 (0.012)
CA1	CA2	1.498	1.521 (0.023)	1.514 (0.016)
CA2	CA3	1.510	1.535 (0.025)	1.535 (0.025)
CA3	CA4	1.534	1.535 (0.001)	1.527 (−0.007)
CA4	CA5	1.514	1.533 (0.019)	1.529 (0.015)
CA5	CA6	1.525	1.534 (0.009)	1.527 (0.002)
CA6	CA7	1.493	1.534 (0.041)	1.527 (0.034)
CA7	CA8	1.513	1.534 (0.021)	1.527 (0.014)
CA8	CA9	1.503	1.534 (0.031)	1.528 (0.025)
CA9	CA10	1.520	1.534 (0.014)	1.528 (0.008)
CA10	CA11	1.475	1.534 (0.059)	1.528 (0.053)
CA11	CA12	1.512	1.530 (0.018)	1.524 (0.012)
CC	OEB	1.442	1.473 (0.031)	1.440 (−0.002)
OEB	CB1	1.334	1.356 (0.022)	1.353 (0.019)
CB1	OB	1.213	1.225 (0.012)	1.215 (0.002)
CB1	CB2	1.508	1.524 (0.016)	1.513 (0.005)
CB2	CB3	1.503	1.537 (0.034)	1.532 (0.029)
CB3	CB4	1.524	1.536 (0.012)	1.527 (0.003)
CB4	CB5	1.502	1.534 (0.032)	1.525 (0.023)
CB5	CB6	1.522	1.534 (0.012)	1.527 (0.005)
CB6	CB7	1.508	1.535 (0.027)	1.527 (0.019)
CB7	CB8	1.529	1.534 (0.005)	1.528 (−0.001)
CB8	CB9	1.504	1.535 (0.031)	1.528 (0.024)
CB9	CB10	1.518	1.534 (0.016)	1.528 (0.010)
CB10	CB11	1.491	1.534 (0.043)	1.528 (0.037)
CB11	CB12	1.515	1.530(0.015)	1.525 (0.010)
CC	CG	1.505	1.538 (0.033)	1.542 (0.037)
CG	OEG	1.437	1.470 (0.033)	1.438 (0.001)
OEG	CG1	1.348	1.353 (0.005)	1.360 (0.012)
CG1	OG	1.184	1.224 (0.040)	1.214 (0.030)
CG1	CG2	1.524	1.518 (−0.006)	1.514 (−0.010)
CG2	CG3	1.539	1.540 (0.001)	1.535 (−0.004)
CG3	CG4	1.531	1.538 (0.007)	1.528 (−0.003)
CG4	CG5	1.505	1.535 (0.030)	1.525 (0.020)
CG5	CG6	1.533	1.535 (0.002)	1.527 (−0.006)
CG6	CG7	1.519	1.535 (0.016)	1.527 (0.008)
CG7	CG8	1.525	1.535 (0.010)	1.528 (0.003)
CG8	CG9	1.507	1.534 (0.027)	1.528 (0.021)
CG9	CG10	1.521	1.534 (0.013)	1.528 (0.007)
CG10	CG11	1.506	1.534 (0.028)	1.527 (0.021)
CG11	CG12	1.533	1.530 (−0.03)	1.525 (−0.008)

[a] All distances are in angstroms.

motions are also large, as are the deviations from standard geometries represented by molecular mechanics force fields (0.05 Å). This discrepancy illustrates the difficulties involved in detailed experimental studies of flexible molecules, and future experimental studies might benefit from support by molecular mechanics modeling studies.

Molecular Dynamics. Preliminary molecular dynamics trajectories of a tripalmitin monomer *in vacuo* using an extended atom approach demonstrated that the initial tuning fork structure of the β-phase bends quickly and stabilizes in a contracted structure where the acyl chains are highly intertangled. This "bird's nest" structure, stabilized by van der Waals interactions, is not unlike the expected structure of simple triglycerides in an oil–air or oil–water interface with the hydrophilic region pointing outward and the three hydrophobic hydrocarbon chains in a parallel arrangement (Small, 1986). Of course, the optimization of van der Waals interactions would not be a driving force for assuming a compact shape in solution simulations since the water molecules would also present a van der Waals field, but it is possible that a similar but slower

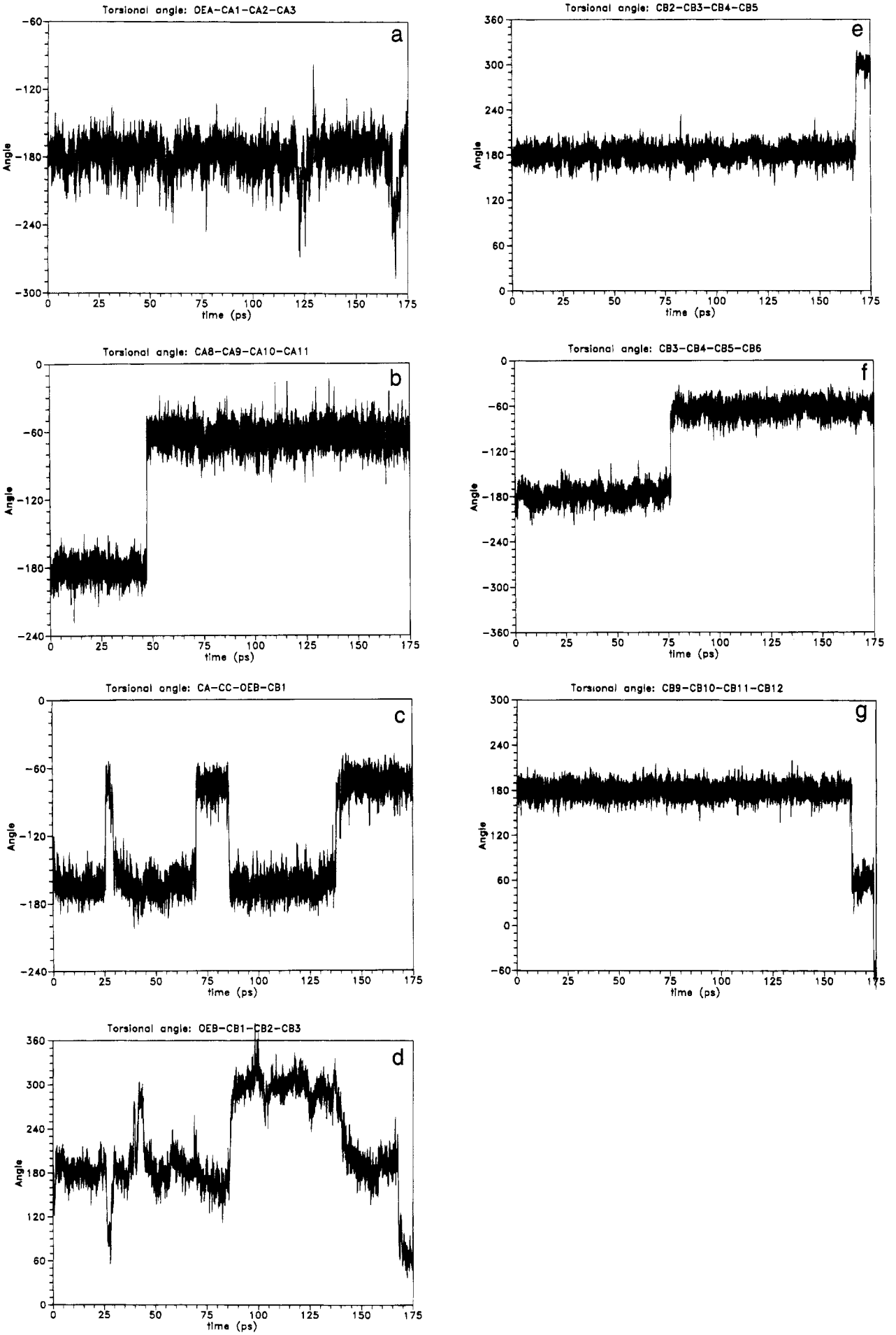

Figure 3. Histories describing transitions of torsional angles over the entire trajectory.

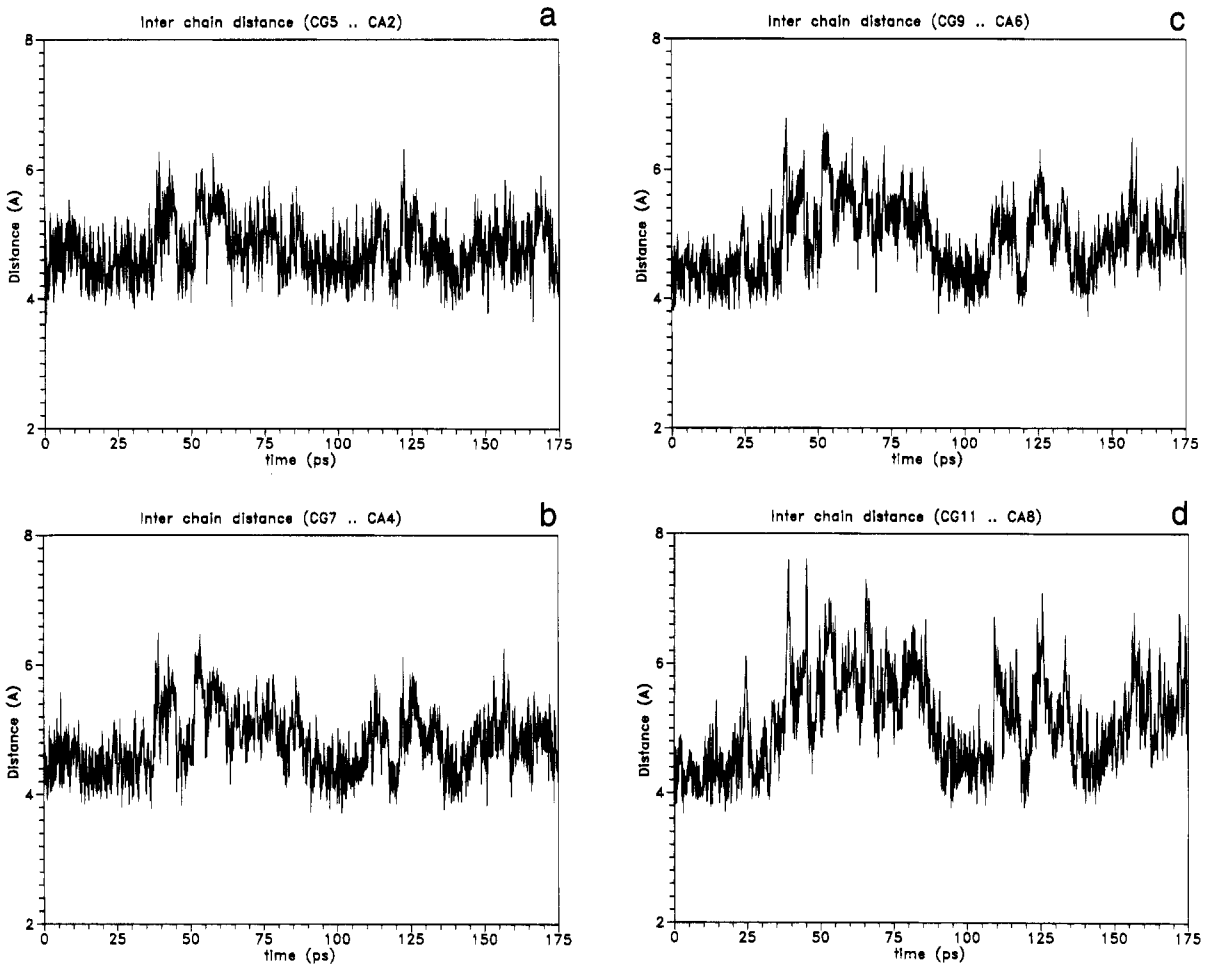

Figure 4. Interchain distances between close atom pairs on the two parallel hydrocarbon chains.

contraction might occur due to entropic forces to reduce the structuring of water molecules around the highly hydrophobic hydrocarbon chains.

In the solution simulation, the trilaurin contraction was much slower and did not proceed to the same extent in the simulated time as it did for tripalmitin *in vacuo*. At no point were all three hydrocarbon chains in van der Waals contact. Likewise, torsional transitions were rare; such transitions occurred in only seven torsional angles: two in the α-strand and the rest in the single, and thus more mobile, β-strand (see Figure 3). The torsional transitions close to the chiral center (Figure 3a,c,d) displayed a tendency to be less abrupt than transitions from the middle and the ends of the strands (Figure 3b,e–g). This difference is presumably due to the frictional drag resulting from local steric constraints. For comparison, an additional trajectory *in vacuo* was calculated to determine the effects of the frictional drag of the water. Surprisingly, this vacuum simulation also exhibited transitions in seven torsional angles, with only a weak tendency toward larger rms fluctuations in the torsional angles. Since this *in vacuo* all-atom trilaurin simulation exhibited a more restricted conformational behavior than the preliminary extended atom tripalmitin simulation, we investigated the force field in more detail. The energy barrier to a torsional transition, as represented by *n*-butane, was calculated to be 4.2 kcal·mol^{-1} and thus in good agreement with the quantum mechanical estimate of 3.36 kcal·mol^{-1} made by Bartell (1977), indicating that the conformational flexibility of trilaurin should be reasonably well reproduced in these simulations.

The parallel arrangement with the α- and γ-strands in van der Waals contact was apparently very stable and was preserved throughout the 175 ps simulation. The arrangement considerably dampened torsional transitions in both strands. Only where the γ-strand ends, leaving the end propyl group of the α-strand essentially free of van der Waals restrictions, did the conformational flexibility of the α-strand increase as indicated by the transitions of the CA8–CA9–CA10–CA11 torsional angle. Atomic motions in the α- and γ-strands were highly correlated, as indicated by the interchain distances between close atom pairs illustrated in Figure 4. Even near the ends of the strands, where the motions have larger magnitudes, they are highly correlated (Figure 4c,d). The approximate end-to-end distance, measured as the end-methyl group to end-methyl group distance, decreased throughout the first part of the simulation until shortly after 100 ps (Figure 5), after which time this distance stabilized and did not further decrease during the remainder of the simulation. The simulation was terminated at 175 ps, since the time scale for torsional kinking events could easily be in the microsecond time scale, beyond available computer resources.

Figures 6–9 illustrate examples of atomic pair distribution functions $g(r)$ (Rossky and Karplus, 1977) for water molecules at a given interatomic distance from selected atoms in the trilaurin solute

$$g(r) = \frac{1}{4\pi\varrho^2}\frac{dN(r)}{dr} \qquad (2)$$

where ϱ is the bulk water number-density. Key values are listed in Table 2. The pair distribution functions for the CA12 and CB12 methyl end groups (Figure 6)

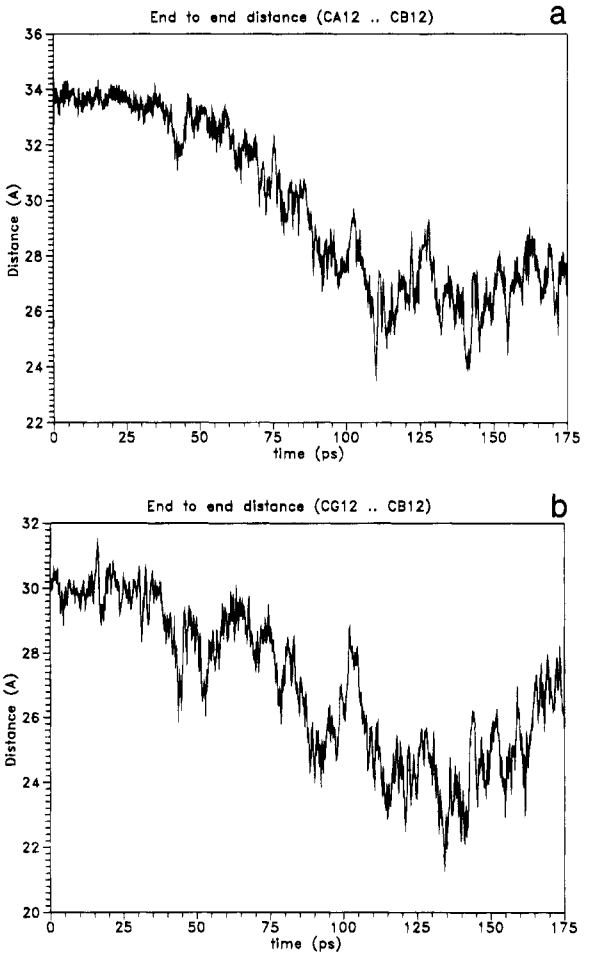

Figure 5. End-to-end distances in the trilaurin solute.

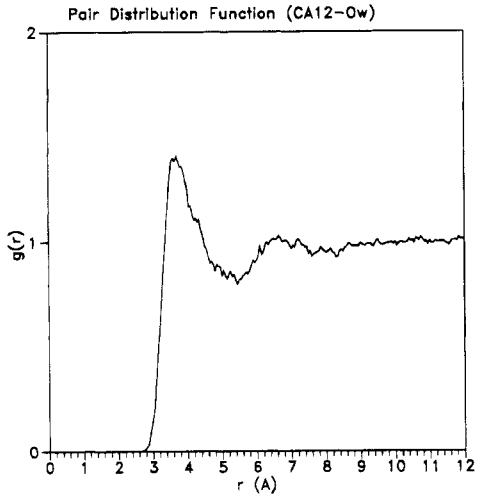

Figure 6. Example of a water oxygen–methyl end group pair distribution function.

exhibited typical nonpolar solvation behavior with a first peak at 3.7 Å corresponding to van der Waals contact and with about 18 near neighbors integrated out to the first minimum at 5.5 Å. The CG12 methyl end group distribution function differed from the others somewhat, with a lower first maximum, reflecting the fact that it is in van der Waals contact with the α-chain, and thus a part of the space of its first solvation shell is occupied and has only about 14 close neighbors. For the midchain solute atoms such as CA7, CB7, or CG7 (Figure 7), in going from methyl end groups to methylene midchain groups, the first peak in $g(r)$ is broadened considerably and is centered about 4.6 Å, while the first

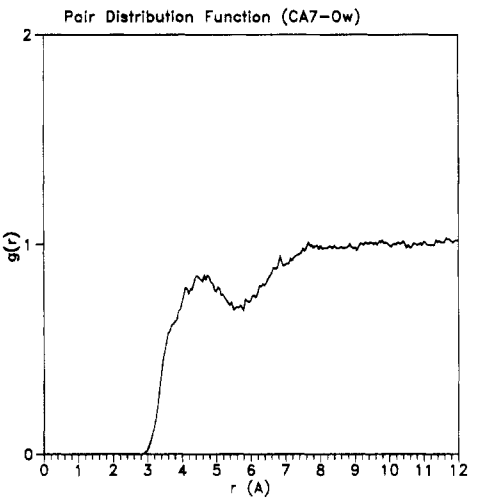

Figure 7. Example of a water oxygen–midchain methylene group pair distribution function.

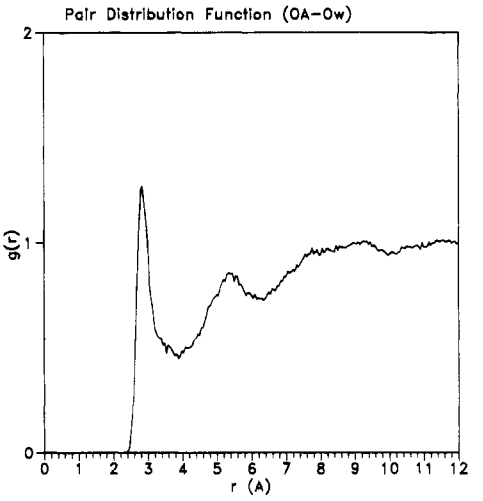

Figure 8. Example of a water oxygen–carbonyl oxygen pair distribution function.

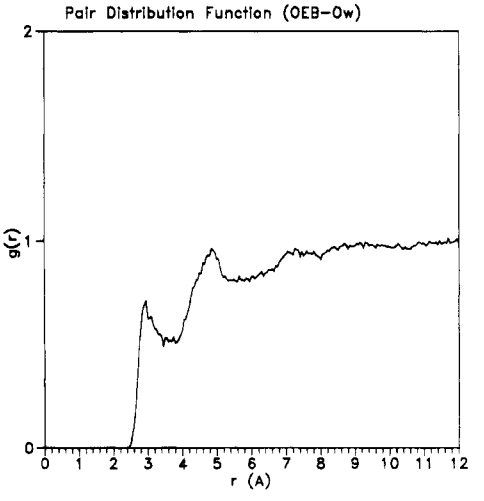

Figure 9. Example of a water oxygen–ester oxygen pair distribution function.

minimum has moved up to about 5.8 Å. The numbers of closest neighbors are about 20 for CB7 on the free B-chain and about 16 for CA7 and CG7 on the parallel α- and γ-chains. Because of the decreased solvent-accessible surface, the first peaks of the latter two curves (Figure 7) do not even reach bulk density. Figure 8 shows an example of the water oxygen pair distribution functions around the carbonyl oxygen atoms OA,

Table 2. Characteristics of the Atomic Pair Distribution Functions for Water Oxygen Atoms around Various Atoms of the Triluarin Solute[a]

atom	max	$g(r)$	min1	min2	I_0^{min1}
CA12	3.7	1.4	5.5		18.1
CB12	3.8	1.5	5.5		18.7
CG12	3.7	1.1	5.3		14.1
CA7	4.7	0.9	5.8		16.0
CB7	4.5	1.1	5.8		20.1
CG7	4.9	0.8	5.8		15.4
OA	2.9	1.3	3.9	6.4	3.8
OB	2.8	1.3	4.0		5.3
OG	2.8	1.5	4.0	6.2	5.2
OEA	3.3	0.5	3.5	5.6	1.2
OEB	3.0	0.7	3.5	~5.6	1.8
OEG	2.9	0.5	3.5	5.3	1.3

[a] All distances are in angstroms.

OB, and OG. In contrast to the pair distribution functions around the hydrophobic nonpolar atoms, these distributions display hydrophilic hydrogen-bonding behavior. Around the carbonyl oxygens, the first peaks are located at approximately 2.8 Å, and the first minima are located at approximately 4.0 Å, both much smaller values than for the nonpolar atoms. The integral of the curves out to the first minimum gives five nearest neighbors around OB and OG and four nearest neighbors around OA. The values indicate that they all have saturated hydrogen-bonding capacity but also non-hydrogen-bonded nearest neighbors. The pair distribution functions around OA and OG both have significant second peaks, with the OA second peak being most pronounced, indicating some long-range structuring with the potential energy functions used. The pair distribution functions around the ester oxygens in the glycerol residue are all perturbed (see Figure 9) with the first peak of these curves significantly distorted, not reaching bulk density, partially due to the proximity of other groups in this crowded region of the trilaurin solute and partially due to the slightly lower partial charge assigned to the ester oxygen (−0.4) compared to the partial charge assigned to the carbonyl oxygen (−0.45). When integrating these probability functions out to the first minimum at 3.5 Å, the single-strand OEB group has 1.8 nearest neighbors, whereas OEA and OEG have 1.2 and 1.3 nearest neighbors, respectively. All of these distributions have well-defined second minima.

The various functional groups of the trilaurin solute also impose orientational order or structuring upon the closest neighbor water molecules. Figures 10−12 show examples of the orientational distributions $P(\cos\theta)$ of water molecules in the first solvation shell (defined by radii of 3.5 Å for polar solute atoms and 5.5 Å for nonpolar solute atoms) (Rossky and Karplus, 1977). These distribution functions are the integrally normalized probability of finding an angle θ between each of the O−H bond vectors in the water molecules and the vector defined by the line from the selected solute atom to the oxygen of the same water molecule. The orientational behavior around the methyl end groups of the solute (Figure 10) is typical for hydrophobic solvation (Rossky and Karplus, 1977), with a peak at +1.0 indicating a tendency for one of the hydrogen atoms to point directly away from the nonpolar group, which avoids the sacrifice of hydrogen bonds. The peak around −0.2 to −0.7 is a consequence of the tetrahedral molecular geometry of the rigid TIP3P water molecules; if one of the hydrogens is pointing directly away from

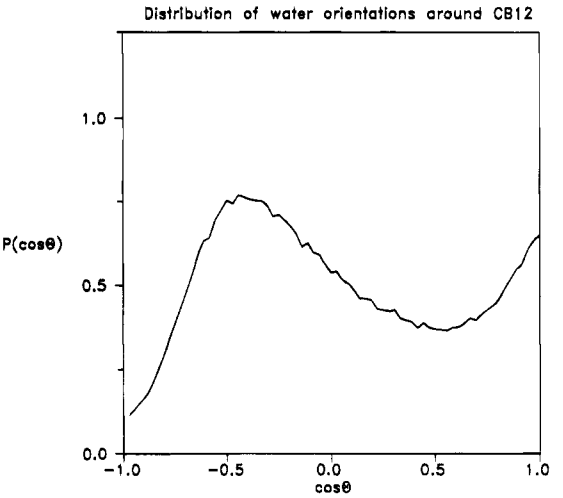

Figure 10. Example of the orientational distribution of water molecules around one of the methyl end groups of the solute.

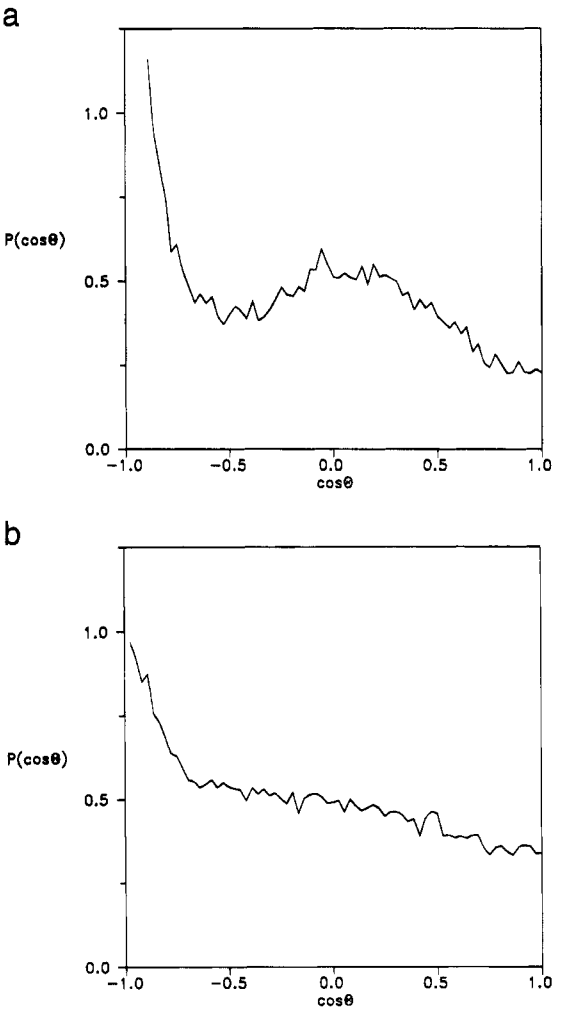

Figure 11. Orientational distributions of water molecules around the carbonyl oxygen atoms of the solute.

the methyl group, the other water O−H bond must make a tetrahedral angle ($\cos\theta = -0.33$) with the C−O vector. The deep minimum at −1.0 indicates that there is little probability of a hydrogen atom pointing directly at the methyl group, a situation which would, however, be energetically favorable close to large hydrophobic surfaces since under those circumstances only one hydrogen bond would be lost (Lee et al., 1984). The cost of the orientational structuring of water is entropic, as the configurational freedom of the water molecules is restricted. The most pronounced difference between the

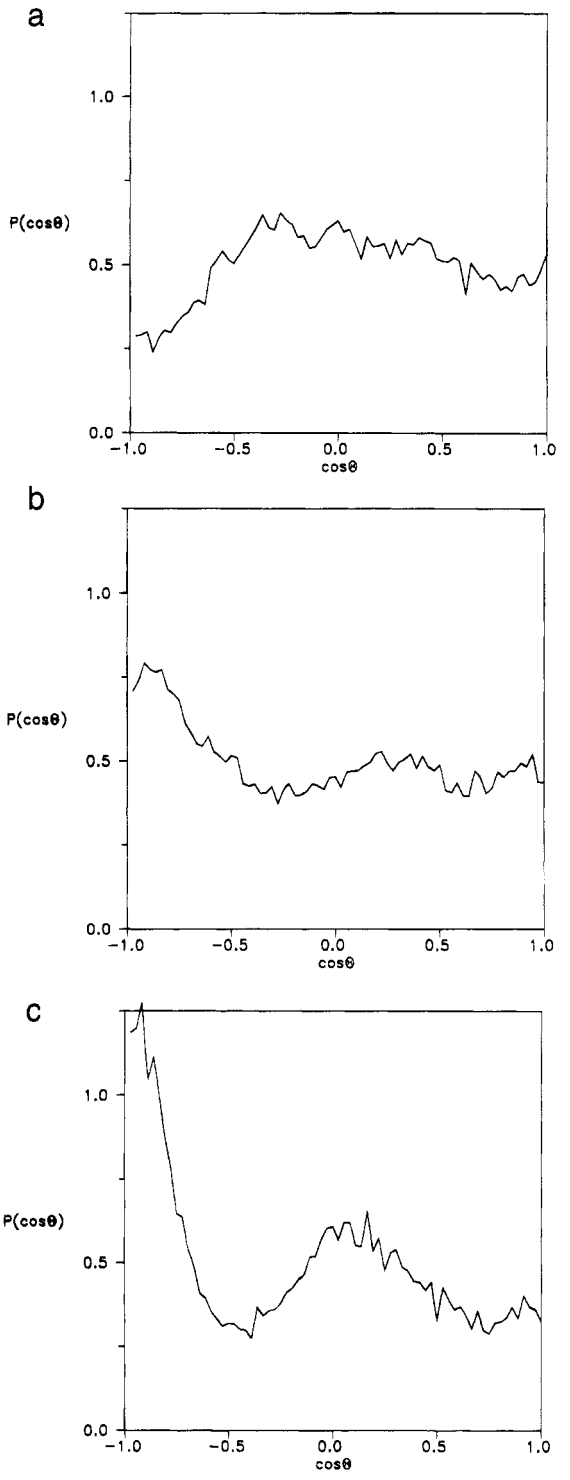

Figure 12. Orientational distributions of water molecules around the ester oxygen atoms of the solute: (a) OEA; (b) OEB; (c) OEG.

distributions for water molecules around the midchain solute methylene groups and those observed around the methyl end groups is an overall "flattening" of the curves. This flattening is caused by a higher probability at $\cos\theta = -1.0$, which indicates that the situation where one O−H bond points directly at the solute atom is more probable for these groups, due to the more extensive hydrophobic surface area. This result is in good agreement with the theory of water structuring about larger hydrophobic groups (Lee et al., 1984). The orientational distribution functions around the hydrophilic carbonyl oxygens (Figure 11a) display typical hydrogen-bond-acceptor behavior. The strong peak at −1.0 indicates that one of the hydrogen atoms of the neighboring water molecules is essentially pointing directly at the carbonyl oxygen atom. The broad secondary peak again results from the tetrahedral geometry of the TIP3P water molecules. The orientational distribution curve about the OB carbonyl oxygen (Figure 11b) is perturbed and exhibits only weak hydrogen-bonding behavior, with a preference for the water molecules to have one hydrogen atom pointing directly at the carbonyl oxygen. The reason for this deviation is not clear since the carbonyl oxygen atom on the single β-strand in principle should be more exposed to the waters than the others. The orientational distributions around the ester oxygen atoms (see Figure 12) are very diverse, with the distribution around OEG showing strong hydrogen-bonding characteristics, the distribution around OEB showing weak hydrogen-bonding characteristics, and the distribution around OEA showing almost no orientational preference but with a minimum at −1 presumably perturbed by adjacent nonpolar groups.

A search was made for any change in water arrangements during "opening" events of the two parallel chains, especially the type of water-separated arrangement reported by Pangali et al. (1979a,b) when analyzing the water structure around two argon atoms in aqueous solution. Those workers found two relatively stable configurations for the hydrophobic spheres: van der Waals contact and a configuration in which each sphere sits in its own hydrophobic water solvation cage, with one water molecule partially fitting in between the spheres. This situation corresponds in principle to an opening event in which pairs of water molecules are forming hydrogen bonds passing perpendicularly between the hydrogen chains. Although such an arrangement is not the most favorable energetically, most time should be spent in this configuration due to the shape of the energy wells. We found no clear evidence of such a solvent-separated configuration, which may be due to the larger "cylinder" radius of the hydrocarbon chains or to inadequate statistical sampling caused by the rare opening events.

Conclusions. From these simulations it would seem that the characteristic crystalline tuning fork geometry for triglycerides is not the preferred conformation in aqueous solution. The slow drift away from the starting structure in the present simulations would imply that the molecule is drifting toward an alternate conformation more compatible with an aqueous environment. It is entirely possible that the molecule might eventually adopt a compact globular type structure like that observed in the vacuum minimization or a structure like that observed by Yan et al. (1994) with all three chains parallel, to minimize water−lipid surface contacts. However, the time scale for such a reorganization might be very much longer than can be conveniently simulated using present computers. For this reason, it is impossible to say whether the leveling off in the decrease in rms end-to-end distance is an indication of having reached a final equilibrium structure or whether slow activated transitions might lead to a further decrease in the surface to volume ratio for the molecule. On an extremely long time scale such as that in most experiments, it is also quite possible that the triglyceride is flexible, with no single well-defined conformation but rather a number of interchanging structures, as has been observed for other lipids (Raghavan et al., 1992; Venable et al., 1993). It would seem likely from these simulations, however, that the structure of triglycerides at a fat globule−water interface may deviate significantly from the crystal structure.

ACKNOWLEDGMENT

All molecular drawings were made using the program MoleCast (S. B. Engelsen, A. Münther, and K. Rasmussen; MoleCast is an unpublished Pascal program available from K. Rasmussen, Chemistry Department A, The Technical University of Denmark, DK-2800 Lyngby, Denmark). This work was supported by a grant from the National Dairy Promotion and Research Board and by Hatch Project 143-7440. S.B.E.'s stay at the Institute of Food Science, Cornell University, was partially supported by The Danish Research Academy, The Carlsberg Foundation, The Otto Mønsted Foundation, The Thomas B. Thrige Foundation, The COWI Foundation, and The Jorck Foundation. We thank K. Rasmussen for supporting the study with computational resources, for establishing the contact between us, and for helpful comments.

LITERATURE CITED

Allen, M. P.; Tildesley, D. J. *Computer Simulation of Liquids*; Clarenden Press: Oxford, U.K., 1987.

Bartell, L. S. Representations of Molecular Force Fields. 3. On Gauche Conformational Energy. *J. Am. Chem. Soc.* **1977**, *99*(10), 3279.

Briggs, J. M.; Nguyen, T. B.; Jorgensen, W. L. Monte Carlo Simulations of Liquid Acetic Acid and Methyl Acetate with the OPLS Potential Functions. *J. Phys. Chem.* **1991**, *95*, 3315–3322.

Brooks, B. R.; Bruccoleri, R. E.; Olafson, B. D.; States, D. J.; Swaminathan, S.; Karplus, M. CHARMM: A Program for Macromolecular Energy, Minimization, and Dynamics Calculations. *J. Comput. Chem.* **1983**, *4* (2), 187–217.

Brooks, C. L.; Karplus, M.; Pettitt, B. M. *Proteins: A Theoretical Perspective of Dynamics, Structure, and Thermodynamics*; Wiley-Interscience: New York, 1988; Vol. 71.

Burkert, U.; Allinger, N. L. *Molecular Mechanics*; ACS Monograph 177; American Chemical Society: Washington, DC, 1982.

De Loof, H.; Harvey, S. C.; Segrest, J. P.; Pastor, R. W. Mean Field Stochastic Boundary Molecular Dynamics Simulation of a Phospholipid in a Membrane. *Biochemistry* **1991**, *30*, 2099–2113.

Egberts, B.; van Gunsteren, W. F.; Berendsen, H. J. C. J. *Chem. Phys.* **1988**, *89*, 3718–3732.

Engelsen, S. B. Ph.D.-Thesis, Chemistry Department A, The Technical University of Denmark, 1991.

French, A. D.; Brady, J. W. *Computer Modeling of Carbohydrate Molecules*; ACS Symposium Series 430; American Chemical Society: Washington, DC, 1990.

Gibon, V.; Blanpain, P.; Norberg, B.; Durant, F. New Data About Molecular Structure of β-Trilaurin. *Bull. Soc. Chim. Belg.* **1984**, *93*, 27–34.

Jensen, L. H.; Mabis, A. J. Refinement of the Structure of β-Tricaprin. *Acta. Crystallogr.* **1966**, *21*, 770–781.

Jorgensen, W. L. Transferable Intermolecular Potential Functions for H_2O, Alcohols, and Other Applications to Liquid Water. *J. Am. Chem. Soc.* **1981**, *103* (2), 335–340.

Larsson, K. The Crystal Structure of the β-Form of Trilaurin. *Ark. Kemi* **1964**, *23* (1), 1–15.

Lee, C. Y.; McCammon, J. A.; Rossky, P. J. The Structure Liquid H_2O at an Extended Hydrophobic Surface. *J. Chem. Phys.* **1984**, *80*, 4448–4455.

McCammon, J. A.; Harvey, S. C. *Dynamics of Proteins and Nucleic Acids*; Cambridge University Press: Cambridge, U.K., 1987.

Mulder, H.; Walstra, P. *The Milk Fat Globule*; Commonwealth Agriculture Bureaux, Farnham University Press: Cambridge, U.K., 1987.

Niketic, S. R.; Rasmussen, K. *The Consistent Force Field (Lecture Notes in Chemistry, Vol. 3)*; Springer Verlag: Berlin, 1977.

Nyholm, P. G.; Pascher, I. *Biochemistry* **1993**, *32*, 1225–1234.

Nyholm, P. G.; Pascher, I.; Sundell, S. *Chem. Phys. Lipids* **1990**, *52*, 1–10.

Pangali, C.; Rao, M.; Berne, B. J. A Monte Carlo Simulation of the Hydrophobic Interaction. *J. Chem. Phys.* **1979a**, *71* (7), 2975–2981.

Pangali, C.; Rao, M.; Berne, B. J. Hydrophobic Hydration Around a Pair of Apolar Species in Water. *J. Chem. Phys.* **1979b**, *71* (7), 2982–2990.

Pastor, R. W.; Venable, R. M.; Karplus, M. Brownian Dynamics Simulation of a Lipid Chain in a Membrane Bilayer. *J. Chem. Phys.* **1988**, *89*, 1112–1127.

Pastor, R. W.; Venable, R. M.; Karplus, M. Model for the Structure of the Lipid Bilayer. *Proc. Natl. Acad. Sci. U.S.A.* **1991**, *88*, 892–896.

Raghavan, K.; Reddy, M. R.; Berkowitz, M. L. A Molecular Dynamics Study of the Structure and Dynamics of Water Between Dilauroylphosphatidylethanolamine Bilayers. *Langmuir* **1992**, *8*, 233–240.

Rasmussen, K. *Potential Energy Functions in Conformational Analysis (Lecture Notes in Chemistry, Vol. 37)*; Springer Verlag: Berlin, 1985.

Rossky, P. J.; Karplus, M. Solvation: A Molecular Dynamics study of a Dipeptide in Water. *J. Am. Chem. Soc.* **1977**, *101*, 1913.

Small, D. M. *The Physical Chemistry of Lipids*; Plenum Press: New York, 1986.

Tasaki, K.; McDonald, S.; Brady, J. W. Observations Concerning the Treatment of Long-Range Interactions in Molecular Dynamics Simulations *J. Comput. Chem.* **1993**, *14*, 278–284.

van Gunsteren, W. F.; Berendsen, H. J. C. Algorithms for Macromolecular Dynamics and Constraint Dynamics. *Mol. Phys.* **1977**, *34* (5), 1311–1327.

Venable, R. M.; Zhang, Y.; Hardy, B. J.; Pastor, R. W. Molecular Dynamics Simulations of a Lipid Bilayer and of Hexadecane: An Investigation of Membrane Fluidity. *Science* **1993**, *262*, 223–226.

Verlet, L. Computer "Experiments" on Classical Fluids, I. Thermodynamical Properties of Lennard-Jones Molecules. *Phys. Rev.* **1967**, *159* (1), 98–103.

Watanabe, K.; Klein, M. L. Shape Fluctuations in Ionic Micelles. *J. Phys. Chem.* **1989**, *93*, 6897–6901.

Yan, Z. Y.; Huhn, S. D.; Klemann, L. P.; Otterburn, M. S. Molecular Modeling Studies of Triacylglycerols. *J. Agric. Food Chem.* **1994**, *42*, 447–452.

Received for review May 19, 1994. Accepted July 18, 1994.[⊗]

[⊗] Abstract published in *Advance ACS Abstracts,* September 1, 1994.